
Mathematical Analysis of the Generation of Force and Motion in Contracting Muscle

E. Pate

Department of Mathematics, Washington State University, Pullman, WA 99164
epate@wsu.edu

Key words: myosin, cross-bridge, actin, muscle, model, muscle mechanics

1 Introduction

The forces involved in muscle contraction result from the contractile proteins, myosin and actin. Myosin captures the free energy available from the hydrolysis of adenosine triphosphate (ATP), and via interaction with actin, generates the force and motion necessary for the survival of higher organisms. How this protein-mediated conversion of chemical energy into mechanical energy occurs remains a fundamental, unresolved question in physiology and biophysics. As a problem in thermodynamics, mathematical modeling of this chemomechanical free energy transduction has played an important role in helping to organize the experimental database into a coherent framework. In this chapter, I will discuss basic models that have been used to analyze this really quite remarkable process – the generation of force and motion from a protein-protein interaction involving the ancillary biochemical reaction of nucleotide hydrolysis.

Recent x-ray structures of the protein myosin show that the N-terminus of the protein is composed of a globular motor domain (also termed the catalytic domain) containing the actin- and nucleotide-binding sites. The motor domain is approximately 10 nm in length. An α -helical neck region, approximately 9 nm in length, projects from the motor domain. Skeletal muscle myosin is dimeric with a molecular weight of approximately 520,000. X-ray, electron microscopic, and secondary structure prediction analyses all suggest the region adjacent to the neck is an α -helical, coiled-coil dimerization domain. The terminal portion of this domain aggregates into the thick filaments seen in muscle ultrastructure. Monomeric G-actin is a globular protein with an approximate diameter of 5–6 nm and a molecular weight of approximately 42,000. Under proper conditions, the G-actin monomers aggregate into a helically arranged, F-actin polymer filament.

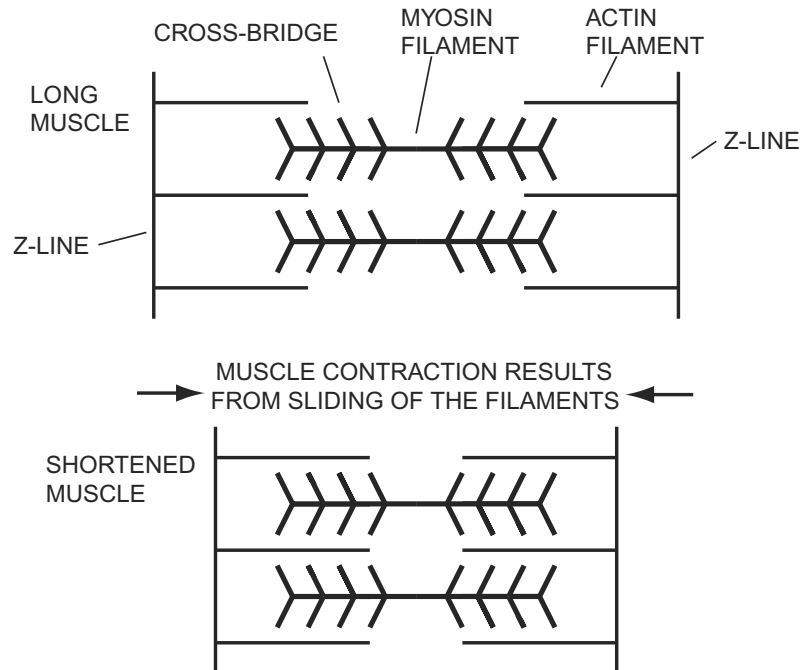


Fig. 1. Cartoon of the relationship between myosin and actin filaments in a sarcomere

The cartoon in Fig. 1 shows the organization of the fundamental contractile unit of muscle, the sarcomere. The sarcomere is an interwoven array of myosin thick filaments, and actin thin filaments. To give relative dimensions, in fast vertebrate skeletal muscle, the myosin filaments are approximately $1.8\mu\text{m}$ in length ($1\mu\text{m} = 10^{-6}\text{m}$). The individual actin filaments are approximately $1\mu\text{m}$ long. Myosin cross-bridges project from the thick filaments and can interact with the thin filaments. The most popular hypothesis at this writing is that the functioning portion of the myosin cross-bridge is the myosin motor domain and the neck, discussed above. The strongest evidence in support of this hypothesis is that the motor domain and neck alone are capable of supporting filament sliding [1]. While interacting with actin, the myosin cross-bridges are capable of producing force and muscle shortening. Early microscopy of muscle demonstrated that shortening does not result from a change in length of the myosin and actin filaments (i.e., a “rubber band” model). Instead, the relatively inextensible filaments slide past each other, with muscle shortening the result of a decrease in the Z-line-to-Z-line distance as diagrammed in Fig. 1 [2, 3]. Other geometrical and size parameters are relevant to understanding our subsequent modeling efforts. Only a few interdigitating filaments have been shown in the planar cartoon of Fig. 1. In skeletal muscle, the thin filament types are arranged in hexagonal arrays around the thick filaments.

The cross-bridges project from the thick filaments in a 6-fold symmetry to accommodate the packing. The rest sarcomere length is approximately $2.5\ \mu\text{m}$. Individual sarcomeres are approximately $1\ \mu\text{m}$ in diameter. They are chained linearly (Z-line to Z-line) in arrays that may be centimeters in length, termed a myofibril. The myofibrils are organized into parallel bundles, termed muscle fibers, which are $50\ \mu\text{m}$ – $100\ \mu\text{m}$ in diameter. With proper magnification, individual muscle fibers can be dissected from skinned muscle preparations (the muscle cell wall has been removed mechanically or chemically). These can then be mounted on a mechanical apparatus specifically designed to measure the mechanical properties of contracting muscle. The muscle fiber has been one of the standard experimental preparations in the study of muscle mechanics. Whole muscle preparations, or single intact muscle cells, have likewise been employed. Parameters given have been for skeletal muscle, and there is variation with muscle type. However, these values remain useful order of magnitude estimates. Unless otherwise noted, magnitudes in the remainder of the chapter will be for fast vertebrate skeletal muscle.

A complete discussion of muscle ultrastructure, myosin structure and mechanics, and the actomyosin biochemical interaction is beyond the scope of this chapter. Excellent detailed reviews are in [4, 5, 6, 7, 8]. The book by Bagshaw [9] is singled out as an outstanding basic introduction to muscle structure, biochemistry, and mechanics. It is highly recommended as a place for interested researchers to start. The lengthier book by Woledge et al. [10] provides a more advanced discussion of the relationship between biochemistry, mechanics, and energetics. The book by Howard [11] discusses myosin function in the broader context of other families of motor proteins, and motor function in the cytoskeleton.

2 A.F. Huxley's Cross-Bridge Model

The experimental observation is that muscle contraction results from the sliding of otherwise relatively inextensible actin filaments, driven by cross-bridges that extend from the myosin filaments and interact with the adjacent actin filaments. Using this as our starting point, we develop the model for muscle cross-bridge function originally presented by A.F. Huxley [12]. Although this model was first presented over 45 years ago, it still contains the fundamental ideas of the overwhelming majority of models that have followed.

The concentration of myosin cross-bridges in muscle is approximately $240\ \mu\text{M}$ [9]. This means that a single 1 cm long muscle fiber, $50\ \mu\text{m}$ in diameter, will contain in excess of 2×10^{12} cross-bridges. The repeat of the myosin cross-bridges projecting from the thick filaments is different from the repeat of the actin monomers that polymerize to form the actin thin filaments. The large number of cross-bridges in the fiber experimental preparation, and the fact that different cross-bridges will see different distances to the nearest actin-binding site (assumed to be a discrete multiple of the 5.5 nm actin

monomer repeat), suggested a continuum model as a first approximation for Huxley [12]. Furthermore, muscle ultrastructure demonstrates that we have an extensive array of interdigitating, parallel filaments. For modeling, this can then be approximated as two infinitely long parallel actin and myosin filaments as shown in the cartoon in Fig. 2. We let x represent the distance between a reference point on a myosin cross-bridge and the nearest actin binding site. We assume a “single-site” assumption where a myosin cross-bridge has a significant probability of interacting with only the nearest actin. With the continuum assumption, the parameter x may be either positive (e.g. x_3 in Fig. 2) or negative (e.g. x_2 in Fig. 2). Shortening with velocity, $v > 0$, will be taken to imply that attached cross-bridges see a decrease in x with time.

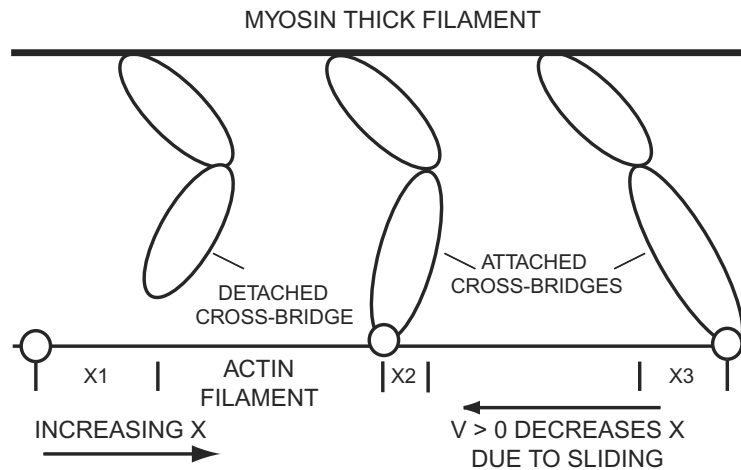


Fig. 2. Cartoon of the Huxley model. For each attached cross-bridge, the reference cross-bridge distortion is idealized as the horizontal distance, x , between the junction of the ellipses representing the cross-bridges and the actin binding site. The value of x increases to the right. Thus $x_2 < 0$ and $x_3 > 0$. Sliding with $v > 0$ decreases the distortion of attached cross-bridges

Let $f(x)$ be the first order (units are s^{-1}), spatially dependent rate of attachment for a myosin cross-bridge that sees the nearest actin binding site at distance x . The quantity, x , is frequently termed the distortion. Let $g(x)$ be the first order detachment rate for a myosin cross-bridge that is attached to an actin binding site at distortion x . Let $n(x, t)$ be the fraction of myosin cross-bridges that see the nearest actin at distortion, x , at time t and are attached. Consider a region of distortions, $[x_0, x_0 + \Delta x]$. The attached fraction in this domain can change by four mechanisms. 1. Detached cross-bridges can attach to actin. 2. Attached cross-bridges can detach. 3. Let the filaments slide relative to each other with velocity, $v > 0$. With the sign conventions of Fig. 2, this implies that attached cross-bridges will experience a decrease in

distortion with time. Equivalently, at position $x_0 + \Delta x$, there will be a flux of attached cross-bridges into the domain $[x_0, x_0 + \Delta x]$. This flux is given by $J(x_0 + \Delta x, t) = \rho v n(x_0 + \Delta x, t)$, where ρ is the density (per unit length) of cross-bridges on the thick filament. 4. A similar effect occurs at x_0 , except that the flux is out of the domain $[x_0, x_0 + \Delta x]$, and $J(x_0, t) = -\rho v n(x_0, t)$. If $n(x, t)$ is the attached fraction, then $1 - n(x, t)$ is the detached fraction. Considering effects 1–4, the balance law giving the time rate of change of the fraction of attached cross-bridges in the domain $[x_0, x_0 + \Delta x]$ is

$$\begin{aligned} \frac{\partial}{\partial t} \int_{x_0}^{x_0 + \Delta x} \rho n(x, t) dx &= \int_{x_0}^{x_0 + \Delta x} f(x) \rho [1 - n(x, t)] dx \\ &+ \int_{x_0}^{x_0 + \Delta x} -g(x) \rho n(x, t) dx \\ &+ J(x_0 + \Delta x) - J(x_0) \end{aligned} \quad (1)$$

i.e. the rate of change = attachment + detachment + flux in – flux out.

Substituting for the definition of J gives a common factor of ρ . Dividing by ρ and applying the mean value theorem for integrals yields

$$\begin{aligned} \frac{\partial n(\xi_1, t)}{\partial t} \Delta x &= f(\xi_2) [1 - n(\xi_2, t)] \Delta x - g(\xi_3) n(\xi_3, t) \Delta x \\ &+ v n(x_0 + \Delta x, t) - v n(x_0, t) \end{aligned} \quad (2)$$

where $x_0 < \xi_1, \xi_2, \xi_3 < x_0 + \Delta x$. The standard procedure of now dividing by Δx and letting $\Delta x \rightarrow 0$, yields a partial derivative in x for the flux, J , terms. Rearranging terms and recognizing that there is nothing special about x_0 so that it can be replaced with x , gives a final balance law of

$$\frac{\partial n(x, t)}{\partial t} - v \frac{\partial n(x, t)}{\partial x} = f(x) [1 - n(x, t)] - g(x) n(x, t). \quad (3)$$

This hyperbolic partial differential equation, along with initial and boundary conditions, describes the evolution of the attached fraction of cross-bridges in time and space. Note that the left-hand side of the equation is the standard material, or convective derivative, given the somewhat non-standard sign convention adopted for positive velocity.

For comparison with experimental muscle data, the model still requires specification of the rate functions, $f(x)$ and $g(x)$. After considerable trial and error, Huxley settled upon the relationship

$$f(x) = \begin{cases} 0, & x > h \\ \frac{f_1 x}{h}, & 0 < x \leq h \\ 0, & x \leq 0 \end{cases} \quad (4a)$$

and

$$g(x) = \begin{cases} 0, & x > h \\ \frac{g_1 x}{h}, & 0 < x \leq h \\ g_2, & x \leq 0 \end{cases} \quad (4b)$$

Huxley was primarily interested in frog fast vertebrate muscle. Brokaw [13] suggested parameter values of $f_1 = 65 \text{ s}^{-1}$, $g_1 = 15 \text{ s}^{-1}$, $g_2 = 313.5 \text{ s}^{-1}$, and $h = 10 \text{ nm}$ as providing a reasonable fit to the observed contraction velocity at 0°C . Rate functions for these values are shown in Fig. 3, and will be used throughout the text when specific values are employed. Muscle is activated by the release of calcium from the sarcoplasmic reticulum. This would imply time-dependent kinetics as a function of calcium concentration. The Huxley model can be viewed as restricting analysis to fully activated conditions.

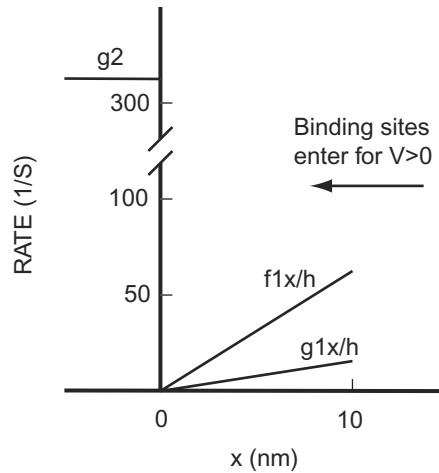


Fig. 3. Kinetic rate functions for cross-bridge attachment and detachment. Values are from Brokaw [13] for frog skeletal muscle

3 Isometric Contraction

Equation (1) is a partial differential equation for cross-bridge function. There are frequently employed experimental protocols that allow the reduction of the model to an ordinary differential equation. The first we will consider is when the muscle, or skinned muscle preparation, is allowed to contract at a fixed length. In this “isometric” mode of contraction, there is no relative sliding of the actin and myosin filaments, $v = 0$, and (1) reduces to the ordinary differential equation in time, with trivial space dependence

$$\frac{dn(x,t)}{dt} = f(x)[1 - n(x,t)] - g(x)n(x,t). \quad (5)$$

Considering the case where all cross-bridges are initially detached, $n(x, 0) = 0$, the differential equation for the fraction attached must be solved in the three regions defined by (4a,b), $x \leq 0$, $0 < x \leq h$, and $x > h$. With $f(x) = 0$ outside the region $0 < x \leq h$, we trivially have $n(x, t) = 0$ for $x \leq 0$ and $x > h$.

Combining the solution of

$$\frac{dn(x, t)}{dt} = \frac{f_1(x)}{h} [1 - n(x, t)] - \frac{g_1(x)}{h} n(x, t), \quad n(x, 0) = 0, 0 < x \leq h, \quad (6)$$

with the zero solution outside this domain, the solution for isometric contraction is given by

$$n(x, t) = \begin{cases} \frac{f_1}{f_1 + g_1} \{1 - e^{-(f_1 + g_1)x/h}\}, & 0 < x \leq h, \\ 0 & x \leq 0, x > h. \end{cases} \quad (7)$$

Several observations are relevant. For large time,

$$\lim_{t \rightarrow \infty} n(x, t) = \frac{f_1}{f_1 + g_1} \quad \text{for } 0 < x \leq h, \text{ see Fig. 4a.} \quad (8)$$

However, this equilibrium distribution is not reached uniformly. From (7), the time constant for the approach to equilibrium, $(f_1 + g_1)x/h$, is greater for larger x . Cross-bridges with distortions of $x \approx h$ attach significantly faster than cross-bridges with $x \approx 0$. Thus one of the fundamental consequences of the Huxley model is that all cross-bridges are not equal as far as reaction kinetics, and ensuing force production, are concerned.

The function of attached cross-bridges is to produce mechanical force. We have solved for the fraction of attached cross-bridges for a model of two infinitely long parallel filaments. To define the force produced in functioning muscle, the attached fraction must be related to the actual physical system of interdigitating thick and thin filaments. Gordon and co-workers [14] experimentally demonstrated a linear decrease in muscle force with a decrease in thick/thin filament overlap (i.e. an increase in muscle length, see Fig. 1). This implies that the cross-bridges in a sarcomere on individual filaments sum in parallel to produce force. Additionally, we need a mathematical constitutive relationship for the force of an attached cross-bridge. The important experimental observation comes from force changes observed in actively contracting muscle subjected to rapid length changes. The idea is to impose a small length change to the muscle sufficiently rapidly such that significant cross-bridge attachment or detachment does not occur during the length perturbation. Thus one is measuring the mechanics of already attached cross-bridges. If Δt is the time during which the length perturbation is completed, this is equivalent in the Huxley model to requiring $\Delta t \ll (f_1 + g_1)^{-1}$ for stretch, or $\Delta t \ll (f_1 + g_2)^{-1}$ for releases. Experimental data [15] show that for either rapid stretches or rapid releases, the change in mechanical force is linearly

proportional to the change in muscle length. This led Huxley to postulate that attached cross-bridges produce force as linear, Hookean springs. Using the notation of Huxley [12], the force produced by an attached cross-bridge with distortion, x , is kx , where k is the elastic force constant. For a muscle with uniform cross-sectional geometry, let A be the cross-sectional area, m be number of cross-bridges per unit volume that can interact with actin, ℓ be the distance between myosin sites and s be the sarcomere length. Then the tension $T(t)$ produced is given by $A(s/2)x$ (average force per cross-bridge), or

$$T(t) = \frac{Asm}{2\ell} \int_{-\ell/2}^{\ell/2} n(x,t)kx dx . \quad (9)$$

Myosin filaments are bipolar, with the two ends connected in series. Under conditions of no filament sliding (isometric), each half sarcomere must produce the same force. Thus the requirement of the factor, $s/2$. Due to the fact that muscle preparations are of different diameters, experimental data are generally normalized in terms of force/unit cross-sectional area. Huxley additionally noted that if a myosin cross-bridge has a significant probability of interacting with only the nearest actin binding site (single-site assumption), the integral on $[-\ell/2, \ell/2]$ in (9) can be replaced with a more general integral on $(-\infty, \infty)$, and the tension per unit area, $P(t) = T(t)/A$ is

$$P(t) = \frac{ms}{2\ell} \int_{-\infty}^{\infty} n(x,t)kx dx . \quad (10)$$

Letting $n(x,t)$ be defined by the cross-bridge distribution for isometric conditions, (7), substituting into (10), and evaluating the integral, gives

$$P(t) = \frac{mksh^2}{4\ell} \left(\frac{f_1}{f_1 + g_1} \right) \left\{ 1 + \frac{2}{(f_1 + g_1)t} e^{-(f_1 + g_1)t} - \frac{2}{[(f_1 + g_1)t]^2} \left(1 - e^{-(f_1 + g_1)t} \right) \right\}, \quad (11)$$

and

$$\lim_{t \rightarrow \infty} P(t) = \frac{mksh^2}{4\ell} \left(\frac{f_1}{f_1 + g_1} \right) . \quad (12)$$

is the final steady-state value of isometric tension, generally represented by P_0 .

Protocols involving rapid length changes allow definition of another useful characterization of cross-bridge behavior in actively contracting muscle. Consider the case where a muscle is rapidly stretched by an amount δx per half sarcomere. In other words, each pair of parallel filaments shifts relative to each other by amount δx , again without significant cross-bridge attachment or detachment. Let $S(t)$, termed the mechanical stiffness of the muscle, be the change in force divided by the change in length. Then

$$S(t) = \frac{ms}{2\ell} \left\{ \int_0^h n(x,t)k(x+\delta x)dx - \int_0^h n(x,t)kx dx \right\} / \delta x . \quad (13)$$

with

$$\lim_{\delta x \rightarrow 0} S(t) = \frac{mks}{2\ell} \int_0^h n(x,t)dx . \quad (14)$$

The integral of $n(x,t)$ in space is just the total fraction of attached cross-bridges as a function of time. Thus in the limit of small length perturbations, with all cross-bridges producing force with the same elastic force constant, $S(t)$ is a measure of total cross-bridge attachment.

4 Isotonic Contraction

The first simplification of the balance law for $n(x,t)$, (1), was motivated by the experimental protocol of isometric contraction, with $v = 0$. Another frequently employed experimental protocol is termed isotonic contraction. Here, an actively contracting muscle is allowed to shorten against a constant force, P . The experimental observation is that after a short initial velocity transient, a steady-state shortening at constant velocity is achieved. Additional details of this protocol and representative experimental data can be found in [16]. A.V. Hill [17] first observed that if P_0 is the isometric tension and steady-state shortening velocity is plotted against normalized tension P/P_0 , the data were well fit by the hyperbolic relationship

$$V = V_{\max} \frac{(a/P_0)(1 - P/P_0)}{a/P_0 + P/P_0} . \quad (15)$$

Here V_{\max} is the maximum velocity of shortening and $a/P_0 > 0$ is an additional parameter for the fit. Both V_{\max} and a/P_0 vary with muscle type and species. Equation (15) is termed the Hill equation. The physiological range is the portion of the hyperbola that decreases monotonically in $(P/P_0, V)$ space from $(0, V_{\max})$ to $(1, 0)$, see Fig. 5. This relationship implies that muscle shortening works on a “there’s no free lunch” basis. In order to shorten more rapidly, muscle has to pay the price of a decrease in the force that it can generate. We next investigate the insights the Huxley model provides into the force-velocity relationship.

For constant velocity shortening with $v > 0$, we can assume a steady-state distribution of cross-bridges in time, and the balance law for cross-bridges, (1), reduces to

$$-v \frac{dn(x)}{dx} = f(x) - [f(x) - g(x)]n(x), \text{ with } \lim_{x \rightarrow \infty} n(x) = 0 \quad (16)$$

For $v > 0$, binding sites enter from the right in Fig. 3. Thus it is necessary to solve (16) in the three domains of different rate functions. Using the functional

values for $f(x)$ and $g(x)$ in (4), the solution for $x > h$ is trivially $n(x) = 0$. For $0 < x \leq h$, the differential equation becomes

$$-v \frac{dn(x)}{dx} = \frac{f_1 x}{h} - \left(\frac{f_1 x}{h} + \frac{g_1 x}{h} \right) n(x). \quad (17)$$

For boundary condition, we assume continuity of n at $x = h$. In order to normalize with respect to different length muscles, physiologists usually give shortening velocities in terms of muscle length per unit time. Thus we let $v = (s/2)V$, where s is the sarcomere length. It is also customary to define $\phi = (f_1 + g_1)h/s$. Then the solution for $n(x)$ in the region $0 < x \leq h$ becomes

$$n(x) = \frac{f_1}{f_1 + g_1} \{1 - e^{[(x^2/h^2 - 1)\phi/V]}\}. \quad (18)$$

For $x \leq 0$, the differential equation for n , (17) becomes

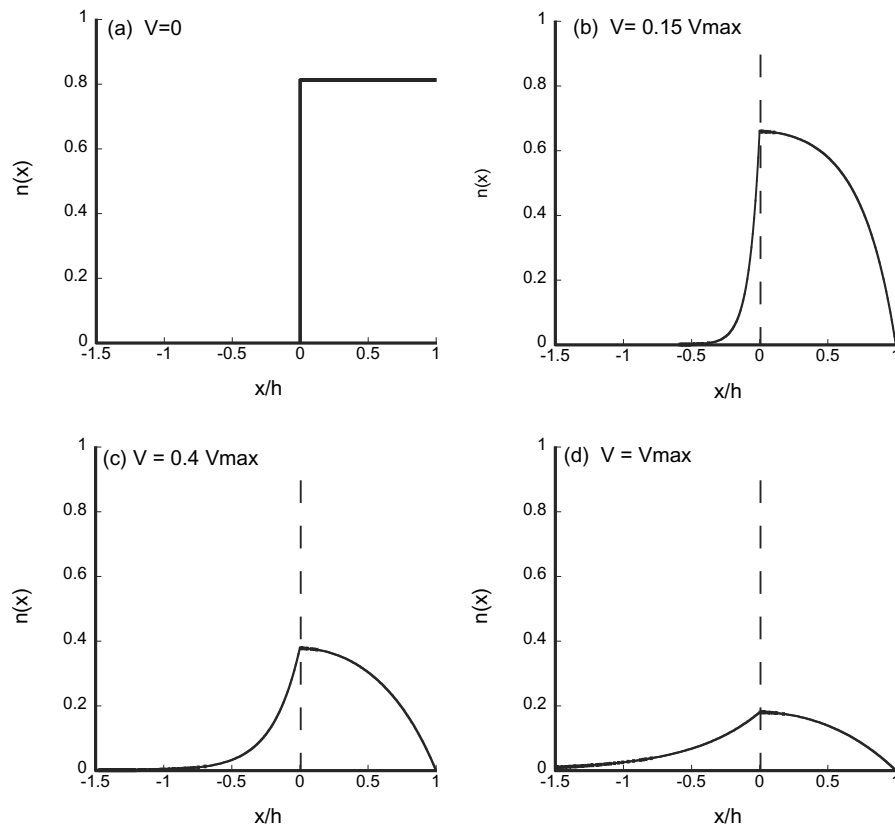


Fig. 4. Cross-bridge distributions, $n(x)$, from (8) (isometric conditions, Panel (a)) and from (18, 20) for shortening at (b) $0.15 V_{\max}$, (c) $0.4 V_{\max}$, and (d) V_{\max}

$$-v \frac{dn(x)}{dx} = -g_2 n(x), \quad (19)$$

with continuity at $x = 0$ as the boundary condition. In terms of parameters V and ϕ the solution is

$$n(x) = \frac{f_1}{f_1 + g_1} [1 - e^{(-\phi/V)}] e^{(2xg_2/sV)}. \quad (20)$$

Figure 4 plots $n(x)$ as a function of shortening velocity. In the Huxley model, attached cross-bridges with $x > 0$ produce a positive force supporting active shortening and will be termed powerstroke bridges. Those with $x < 0$, produce a negative, resistive force to active shortening and will be termed dragstroke cross-bridges. For $V = 0$, there is a spatially uniform distribution of powerstroke cross-bridges and no dragstroke bridges (Fig. 4a). Binding sites enter from the right for $V > 0$. Attachment begins when the distance to an actin binding site satisfies $x \leq h$ and the fraction of attached cross-bridges increases with passage through the powerstroke toward $x = 0$. However, the time of passage decreases with increasing velocity and thus the maximum fraction attached in the region $x > 0$ decreases with increasing velocity (Fig. 4b–d). For $x \leq 0$, the flux term in (1) implies that cross-bridges will be carried into the dragstroke region by work done by powerstroke cross-bridges. More rapid cross-bridge detachment begins when $x < 0$, due to the discontinuity in the off-rate function $g(x)$. However, this off-rate is again finite, and with increasing velocity, cross-bridges translate, on average, further into the dragstroke region before detaching. Increasing shortening velocity decreases the net force from positively strained cross-bridges relative to that produced by negatively strained cross-bridges. It had long been recognized that muscles have a maximum shortening velocity, and as formalized in the Hill relation, (15), the net cross-bridge force at V_{\max} is zero. Huxley's key conceptual insight was that for the first time, he provided a mechanical explanation for the existence of V_{\max} . V_{\max} is simply that velocity at which the negative force produced by the dragstroke cross-bridges exactly balances the positive force produced by the powerstroke cross-bridges.

However, the Hill relation further suggested a specific hyperbolic, functional relationship at intermediate velocities. Inserting the solution for $n(x)$, (18, 20) into the definition of $P(t)$, (11), evaluating the integral, and observing the value of P_0 from (12) gives the relationship

$$P/P_0 = 1 - \frac{V}{\phi} \left(1 - e^{-\phi/V}\right) \left[1 + \frac{1}{2} \left(\frac{f_1}{f_1 + g_1}\right)^2 \frac{V}{\phi}\right]. \quad (21)$$

This transcendental equation relating tension and shortening velocity is the Huxley model equivalent of the hyperbolic Hill equation. Both are plotted in Fig. 5. The figure shows that to within the experimental error, the fits are equivalent. The fundamental difference is that the Hill fit is based upon

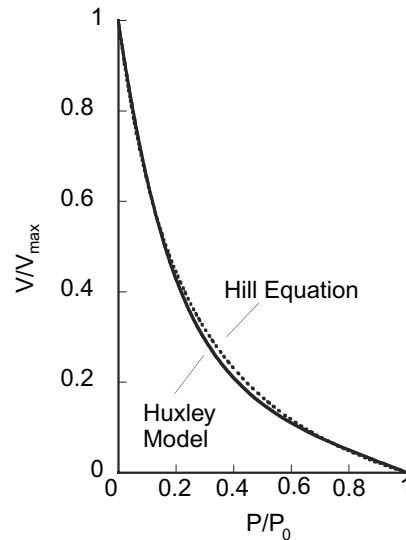


Fig. 5. Force-velocity relationship from the Huxley model (*solid line*) and the Hill equation (*dashed line*). Parameters for the Huxley model are taken from Fig. 3. For the Hill equation, $a/P_0 = 0.25$

heuristic curve fitting of an experimental observation. The Huxley fit follows naturally from the fundamental properties of interacting, linearly elastic cross-bridges.

In his original paper, Huxley also analyzed energy liberation during contraction. Hill [17] suggested that energy liberation (heat + work) increased monotonically with the speed of shortening. Huxley [12] showed that the model also accurately fit the energy liberation data of Hill [17]. However, Aubert [18] later questioned the Hill observation, suggesting instead that energy liberation increased initially with shortening velocity, but for rapid shortening velocities, energy liberation decreased with increasing velocity. More advanced technologies always allow for improved experimental equipment. Hill [19] subsequently agreed that energy liberation decreased at high shortening velocities (greater than $\sim V_{\max}/2$). With current technologies, these remain difficult experiments. Despite its experimental limitations, the energy analysis of Huxley [12] showed for the first time the mathematical framework of how a cross-bridge model can be used to interpret energy liberation. It thus remains extremely informative, and the reader is referred to the original work for details [12]. It should likewise be noted that having developed a model, and then having experimentalists change the experimental data underpinning the model, remains a professional risk for modelers even today.

Since Huxley's original work, a number of modifications have been proposed, while maintaining the same basic conceptual framework. A complete discussion of modeling after 1957 is beyond the scope of this chapter. I limit

discussion to the inclusion of improved modeling of the biochemical cycle and of thermodynamic constraints. The original Huxley model considered a single attached and a single detached state. Lynn and Taylor [20] provided the first widely accepted model of the actin-myosin-ATP biochemical interaction, based upon experimental studies of the isolated proteins in solution, which linked cross-bridge biochemical cycling to cross-bridge muscle mechanics. The model contained five states (two detached, three attached) and is shown in Fig. 6. Forward and reverse transitions are allowed between adjacent states, but the working cycle goes in a clockwise direction.

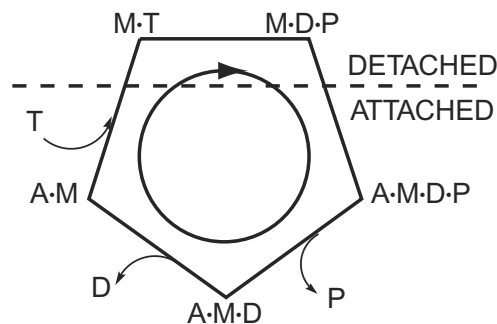


Fig. 6. Kinetic scheme for the actin-myosin-nucleotide interaction. All steps are reversible, but the contractile cycle goes in the clockwise direction. A = actin, M = myosin, T = ATP, D = ADP, and P = orthophosphate. Starting at *upper left*, ATP is hydrolyzed on myosin (in the absence of actin) with a transition to a myosin-hydrolysis products state, M·D·P. The binding to actin yields an A·M·D·P state. P is released first, followed by D, resulting in the A·M, rigor complex. The binding of ATP results in the dissociation of the actomyosin complex into the original M·T state. All states above (*below*) the *dashed line* are detached from (*attached to*) actin. The actual biochemical cycle is more complicated, and the precise determination of all states involved remains unresolved. This cycle can be viewed as common to more complex models (reviewed in [9] and references therein)

The Huxley model can be viewed as lumping the attached states and detached states into single states. If this is the resolution of the experimental data one wishes to explain, this is a valid simplification. On the other hand, inclusion of the entire five-state model allows for the analysis of mechanical effects of variation of substrate, ATP, and hydrolysis products, ADP and phosphate. There is additional evidence suggesting the mechanical and kinetic properties of the individual states have different dependences on the spatial parameter, x (reviewed in [21, 22] and references therein). More realistic biochemical models are necessary to model these types of effects. However, it must also be recognized that additional, distinct states come at a modeling price. For an N-state model, (1) generalizes to a coupled system of N-1 partial differential equations. I note that Huxley [23] demonstrated that a model

containing more than two states could overcome the energy liberation problems of the original two-state model.

Another conceptual advance was the work of Eisenberg and co-workers [21]. In their models, multiple, linearly elastic attached cross-bridge states were assumed with different attached states having different values of distortion for the neutral strain position. In particular, initial attachment was in a weakly attached, low-force, pre-powerstroke state, with subsequent transition into a strongly bound powerstroke attached state, which was mechanically comparable to the attached state in the Huxley model. Considering in greater detail the relationship between thermodynamics and mechanics for linearly elastic cross-bridges, the force produced at distortion, x , for a given state i in a multi-state model was given by $F_i(x) = dG_i(x)/dx$, where $G_i(x)$ is the free energy of the attached state, which is quadratic in x . This is homologous to the relationship in classical physics between a linear spring and its parabolic potential energy as a function of extension, x . Eisenberg and co-workers further observed that if $R_{ij}(x)$ and $R_{ji}(x)$ were the forward and reverse transition rates between states i and j , they could not be thermodynamically independent. They must instead be related by $R_{ij}(x)/R_{ji}(x) = \exp[G_i(x) - G_j(x)]/RT$, where R is the Boltzmann constant and T is absolute temperature. Of the forward rate function, the reverse rate function, and the free energy difference between the two states, the Gibbs relationship implied that only two could be independently specified. The third was then automatically fixed. This condition has been termed “thermodynamic consistency” for cross-bridge models. Additional details are provided in the original references.

5 Transient Simulations

Our discussion of modeling has used two common experimental protocols to reduce the Huxley balance law to ordinary differential equations. The full transient equations have been less frequently employed. They are, for example, required for the modeling of the entire activation, contraction, and relaxation cycle of cardiac muscle. However, the initial, detailed transient application was for analysis of the beating of cilia and flagella. In this system, the motor protein is dynein. It interacts with the microtubule polymer that forms the tail of a flagella or the cilia hair to cause the rhythmic beating motion. Dynein appears to have many mechanical and biochemical characteristics in common with myosin. Accepting myosin-like behavior, the periodic nature of flagellar and ciliary beating requires solution of the full time- and space-dependent equation. Hines and Blum [25, 26] were the first to use finite difference schemes to solve the hyperbolic cross-bridge balance law. These and other numerical schemes can likewise be applied to myosin systems.

Brokaw [13] developed an alternative, probabilistic modeling approach. We discuss his work in greater detail, as it ultimately relates back to the analysis

of evolving experimental protocols in actomyosin systems. In this modeling approach, one starts with the knowledge of the states of all the cross-bridges in a finite ensemble at time, t . For the original Huxley model, this would be whether the cross-bridge is attached or detached. Parallel actin and myosin filaments are assumed. One then increments a small increment in time, δt , to time $t + \delta t$. This is done as follows. For each cross-bridge, the distance, x , to the nearest actin-binding site is calculated. If the cross-bridge is attached, the probability of detachment in the time step, δt is determined. For the Huxley model this is

$$p_d(x) = g(x)[1 - \exp(-B(x)\delta t)]/B(x), \quad \text{where } B(x) = f(x) + g(x). \quad (22)$$

If the cross-bridge is detached, the probability of attachment during a time step, δt is calculated,

$$p_a(x) = f(x)[1 - \exp(-B(x)\delta t)]/B(x). \quad (23)$$

The probability is compared with a computer-generated pseudorandom number and the cross-bridge status (detached or attached) is updated. All remaining cross-bridges are similarly updated. In reality, computational speed is enhanced by generating a table of probabilities as a function of x and then doing a table lookup at each step. The forces generated by all cross-bridges are then balanced against any imposed external load by shifting the modeled actin filament relative to the modeled myosin filament so that the cross-bridge force and imposed load come into balance. Brokaw [27, 28] discusses transition probabilities for models involving more than two states.

The advantage of the probabilistic approach was that it was easy to program, and did not require advanced knowledge of finite difference or other approaches for numerically solving partial differential equations. The disadvantages were that it was a first-order scheme, and that one had to either deal with large ensembles of cross-bridges, or to average multiple simulations with smaller numbers of cross-bridges, in order to eliminate statistical noise. This made the probabilistic scheme computationally more time consuming. However, with massive parallelization on the horizon, and the assumption of independently functioning cross-bridges, this computational speed deficiency may not be the case in the future.

The goal is to use modeling to describe how an individual cross-bridge functions. As noted in Sect. 1, the large numbers of cross-bridges in a muscle fiber justifies the use of a continuum model. The disadvantage of the intact muscle preparation is that the properties of an individual cross-bridge must be deduced from an ensemble average of a very large number of independently functioning cross-bridges that are not synchronized in their chemomechanical cycle. One way to examine better the properties of an individual cross-bridge is to use experimental systems that contain only a few cross-bridges. In this situation, probabilistic models will not be just useful; they will be essential. I describe this application next.

6 Analysis of Systems of Small Numbers of Cross-Bridges

The first experimental protocol that allowed examination of the mechanical properties of small numbers of motor molecules was a reconstituted system of motor proteins termed an *in vitro* assay [29, 30, 31, 32]. In this protocol, as generally employed today, a solution of myosin, or a myosin fragment containing the motor domain, is brought in contact with a nitrocellulose coated glass surface. Individual molecules became fixed to the substrate. The number of motors on the surface can be controlled by the concentration in the solution and the contact time. The solution is then exchanged for one containing polymerized actin filaments and ATP. With proper microscopy, the actin filaments can then be visualized gliding like snakes across a lawn of myosin motors. Gliding velocities are comparable to those observed in whole fiber preparations. Photographs, on-line videos, and additional discussion of *in vitro* assays can be found on the world-wide web at <http://www.mih.unibas.ch/Booklet/Booklet96/Chapter2/Chapter2.html> (Andreas Bremer, Daniel Stoffler and Ueli Aebi), <http://biochem.stanford.edu/spudich/> (James Spudich), and <http://physiology.med.uvm.edu/warshaw/TechspgInVitro.html> (David Warshaw). An additional advantage of this protocol is that it can be used with myosins that do not form filaments (e.g., intracellular myosins involved in organelle transport).

We consider an application of probabilistic models to this experimental setup. As noted previously, relative sliding of the actin filaments will be a balance of cross-bridge forces and any imposed load. The average force produced by a single myosin cross-bridge is in the picoNewton range ($1 \text{ pN} = 10^{-12} \text{ N}$) (reviewed in [5, 7, 8]). There are two imposed loads that need to be considered in the *in vitro* assay. One is viscosity; the other is inertia. Approximating an actin filament to be a cylinder of radius 10 nm, the viscous resistance to sliding along the long axis at a typical velocity of 1000 nm/sec will be only about $1 \text{ fN}/\mu\text{M}$ ($1 \text{ fN} = 10^{-15} \text{ N}$) [33]. The viscous resistance is a factor of 100–1000 less than the force of a *single* cross-bridge, and thus viscous forces will be ignored. For a filament moving through a viscous fluid, the Reynolds number, $\text{Re} = UL/v$, is a dimensionless quantity giving the ratio of inertial to viscous forces. Here U is a velocity scale, L is a length scale and v is the kinematic viscosity of the fluid. Take $U = 1000 \text{ nm/sec}$, $L = 1 \mu\text{m}$, and $v = 0.01 \text{ cm}^2/\text{sec}$ (water). Then $\text{Re} = 10^{-6}$, and inertial force of the filament is even smaller than the already ignored viscous force. In other words, when we update the filament position for a time step, δt , in the probabilistic model, we are in a situation of unloaded filament sliding. After updating the cross-bridges, assume there are $i = 1, \dots, n$ attached cross-bridges with distortions x_i . Then our zero net force requirement is determined by a translation of the actin filament by an amount, δx , which satisfies

$$\sum_{i=1}^n k(x_i - \delta x) = 0, \text{ with solution } \delta x = \left(\sum_{i=1}^n x_i \right) / n. \quad (24)$$

If $n = 0$, no translation is made.

Figure 7 shows representative results from simulations using the Huxley two-state model cross-bridge kinetic scheme, as the number of cross-bridges, N , increases. The graininess of the stepping is evident, although for $N = 50$ it is already dramatically reduced. The other unexpected observation is that the average velocity of sliding increases with cross-bridge number (Fig 7). This has been observed experimentally for myosin [32]. We now consider the factors that determine sliding velocity for a small and a large number of cross-bridges, and show that modeling can demonstrate how the interplay of competing effects offers an explanation for velocity increases with increasing cross-bridge number.

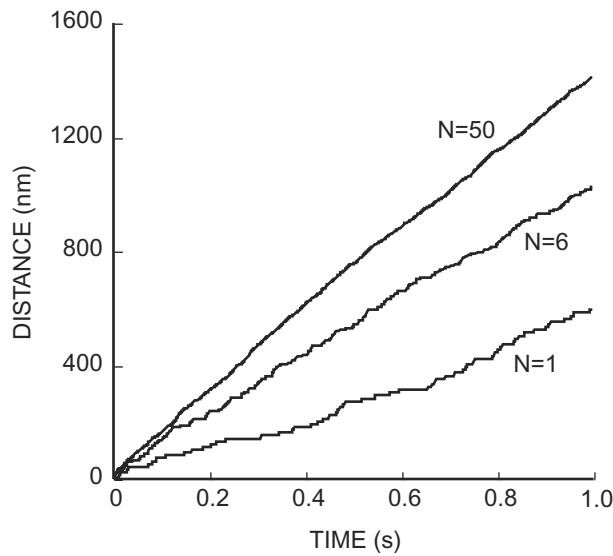


Fig. 7. Sliding distance as a function of time for finite ensembles of Huxley-model cross-bridges. Results for 1, 6, and 50 cross-bridges are shown. Parameters for f_1 , g_1 , g_2 , and h were taken from Fig. 3 (Brokaw [13] model for frog muscle, 0°C)

For the simulations of Fig. 7, myosin cross-bridges were assumed to have the thick filament repeat of 42.9 nm and actin sites a spacing of 10 nm, the powerstroke length. The latter insures retention of single-site, thick-thin filament interaction in even the single cross-bridge, $N = 1$ case, which we consider first. For the parameters used in the simulations, the nearest binding site will be located at $x = h$ after the first step. Using the Huxley kinetic

parameters for frog muscle, (4), cross-bridge attachment will occur with rate $f(10 \text{ nm}) = f_1 = 65 \text{ s}^{-1}$. In the presence of negligible resistive forces, translation of the actin filament by a distance of $\delta x = 10 \text{ nm}$, (24) follows. Detachment then occurs with rate $g(0) = g_2 = 313.5 \text{ s}^{-1}$. The mean velocity of sliding will be the mean cycle rate time the powerstroke length. For independent Poisson attachment and detachment processes, this becomes

$$v = (f(h)^{-1} + g(0)^{-1})^{-1}h . \quad (25)$$

For our simulations, $f(h) \ll g(0)$, ($f_1 \ll g_2$) and to a first approximation,

$$v = f(h)h . \quad (26)$$

For a large number of cross-bridges, the limit as $N \rightarrow \infty$ gives the original Huxley model. Then

$$\begin{aligned} \frac{\partial n(x,t)}{\partial t} - v \frac{\partial n(x,t)}{\partial x} &= -g_2 n(x,t) , \quad x \leq 0 \\ \frac{\partial n(x,t)}{\partial t} - v \frac{\partial n(x,t)}{\partial x} &= \frac{f_1 x}{h} [1 - n(x,t)] - \frac{g_1 x}{h} n(x,t) , \quad 0 < x \leq h \end{aligned} \quad (27)$$

with $n(x,t) = 0$ for $x > h$. In order to properly compare the relative sizes of the terms in our analysis, it is necessary to introduce dimensionless, scaled variables. Let $X = x/h$, $T = g_2 t$ be the dimensionless space and time variables. The dimensionless cross-bridge fraction, $n(x,t) \in [0,1]$, and is already scaled. In terms of the new parameters, the balance law for cross-bridges becomes

$$\begin{aligned} \frac{\partial n(X,T)}{\partial T} - V \frac{\partial n(X,T)}{\partial X} &= -n(X,T) , \quad X \leq 0 \\ \frac{\partial n(X,T)}{\partial T} - V \frac{\partial n(X,T)}{\partial X} &= -RXn(X,T) + HX , \quad 0 < X \leq 1 \end{aligned} \quad (28)$$

Here the dimensionless velocity $V = v/(g_2 h)$, $R = (f_1 + g_1)/g_2$ is the dimensionless ratio of kinetic constants in the powerstroke and dragstroke force regions, and $H = f_1/g_2$. For steady-state contraction $\partial n/\partial T = 0$, resulting again in ordinary differential equations in X . With $n(1) = 0$ and continuity at $X = 0$, the solution becomes

$$\begin{aligned} n_-(X) &= \frac{H}{R} [1 - e^{-R/2V}] e^{X/V} , \quad X \leq 0 \\ n_+(X) &= \frac{H}{R} [1 - e^{R(X^2-1)/V}] , \quad 0 < X \leq 1 \end{aligned} \quad (29)$$

where the \pm subscripts denote the negative and positive distortion region solutions, respectively. The sliding velocity under unloaded conditions will occur when the positive and negative cross-bridge forces balance. With k as the cross-bridge elastic force constant, we require

$$\int_0^1 n_+(X)kXdX + \int_{-\infty}^0 n_-(X)kXdX = 0 \quad (30)$$

Substituting for $n_{\pm}(X)$ and evaluating the integrals, the dimensionless sliding velocity, V , is the solution of the transcendental equation

$$1 - \frac{2V}{R}(1 - e^{-R/2V})(1 + VR) = 0 \quad (31)$$

The parameter $R = (f_1 + g_1)/g_2 = 0.26$ for the Huxley kinetic parameters. Anticipating that the scaled velocity is $O(1)$, we assume a series expansion for V in terms of powers of R ,

$$V = a_0 + a_1R + a_2R^2 + \dots \quad (32)$$

where the a_i are constants. Substitute the power series in R into (31) and expand the exponential term in a Taylor series in $R < 1$. Grouping the terms involving like powers of R , and setting the terms individually to zero, yields a system of algebraic equations that satisfy (31). Solving the equations for the a_i yields

$$V = \frac{1}{2} + \frac{1}{24}R + O(R^2). \quad (33)$$

In terms of dimensioned variables, this becomes (first term only)

$$v = \frac{g_2h}{2}. \quad (34)$$

We can now see the interplay that determines relative sliding velocities at low and high cross-bridge number. For $N = 1$, and the parameters relevant to frog fast skeletal muscle, the rate limiting step for the Huxley for the model is $f(h) = f_1$, the attachment rate at the beginning of the powerstroke. For the case of an infinite number of cross-bridges, the rate-limiting step becomes the detachment rate in the negative force region, $g(x) = g_2$. Due to the magnitudes of f_1 and g_2 , the sliding velocity is greater for a large number of cross-bridges.

Note that other parameter ratios can yield different results as a function of cross-bridge number. For example, if $g_2 \ll f_1 + g_1 < f_1$, then for $N = 1$, detachment, $g(0)$, and not attachment, $f(h)$, now dominates in (25). The mean velocity becomes $v = g_2h$ for the single cross-bridge case. Comparison with the Lymn-Taylor biochemical cycle [20] suggests that this is equivalent to considering a regime in which the concentration of substrate, ATP, is very low [34]. The parameter $R = (f_1 + g_1)/g_2 \gg 1$. The proper expansion for V to solve the transcendental (31) for V is now in powers of $1/R$, and it can be shown that

$$v = \frac{g_2h}{\sqrt{2}}. \quad (35)$$

Thus in this case, the Huxley model predicts that sliding velocity of many cross-bridges will be less than that of a single cross-bridge. Additional details are provided in [34].

In summary, we are now approaching 5 decades after the original work by Huxley. The basic framework of the Huxley model remains the primary foundation for the quantitative interpretation of experimental data. This includes both persons who would claim to be primarily experimentalists and persons who are primarily modelers seeking to add quantitative insight into the experimental database. Although modifications have been made as the experimental database has expanded, the original basic assumptions of elastic attached cross-bridges and spatially dependent cross-bridge kinetics continue to dominate the muscle conversation.

References

1. Toyoshima, Y.Y., S.J. Kron, E.M. McNally, K.R. Niebling, C. Toyoshima, and J.A. Spudich, Myosin subfragment-1 is sufficient to move actin filaments in vitro. *Nature*, 1987. 328: 536–539. [134](#)
2. Huxley, A.F. and R. Niedergerke, Structural changes in muscle during contraction; interference microscopy of living muscle fibres. *Nature*, 1954. 173: 971–973. [134](#)
3. Huxley, H. and J. Hanson, Changes in the cross-striations of muscle during contraction and stretch and their structural interpretation. *Nature*, 1954. 173: 973–976. [134](#)
4. Cooke, R., Force generation in muscle. *Curr Opin Cell Biol*, 1990. 2: 62–66. [135](#)
5. Cooke, R., Actomyosin interaction in striated muscle. *Physiol Rev*, 1997. 77: 671–697. [135](#), [148](#)
6. Taylor, E.W., Mechanism of actomyosin ATPase and the problem of muscle contraction. *CRC Crit Rev Biochem*, 1979. 6: 103–164. [135](#)
7. Geeves, M.A. and K.C. Holmes, Structural mechanism of muscle contraction. *Annu Rev Biochem*, 1999. 68: 687–728. [135](#), [148](#)
8. Holmes, K.C. and M.A. Geeves, The structural basis of muscle contraction. *Philos Trans R Soc Lond B Biol Sci*, 2000. 355: 419–431. [135](#), [148](#)
9. Bagshaw, C.R., *Muscle Contraction*. Second ed. 1993, London, UK: Chapman and Hall, Ltd. x + 155. [135](#), [145](#)
10. Woledge, R., N.A. Curtin, and E. Homsher, *Energetic Aspects of Muscle Contraction*. Monographs of the Physiological Society. Vol. 41. 1985. xiii + 359. [135](#)
11. Howard, J., *Mechanics of Motor Proteins and the Cytoskeleton*. 2001, Sunderland, MA: Sinauer Associates, Inc. xvi+367. [135](#)
12. Huxley, A.F., Muscle structure and theories of contraction. *Prog Biophys Biophys Chem*, 1957. 7: 255–318. [135](#), [136](#), [140](#), [144](#)
13. Brokaw, C.J., Computer simulation of movement-generating cross-bridges. *Biophys J*, 1976. 16: 1013–1027. [138](#), [146](#), [149](#)
14. Gordon, A.M., A.F. Huxley, and F.J. Julian, The variation in isometric tension with sarcomere length in vertebrate muscle fibres. *J Physiol*, 1966. 184: 170–192. [139](#)
15. Huxley, A.F. and R.M. Simmons, Proposed mechanism of force generation in striated muscle. *Nature*, 1971. 233: 533–538. [139](#)
16. Cooke, R., K. Franks, G.B. Luciani, and E. Pate, The inhibition of rabbit skeletal muscle contraction by hydrogen ions and phosphate. *J Physiol*, 1988. 395: 77–97. [141](#)
17. Hill, A.V., The heat of shortening and dynamic constraints of muscle. *Proc. Royal Soc. London. Series B. Biol. Sci.*, 1938. 126: 297–318. [141](#), [144](#)

18. Aubert, X., *Le couplage energetic de la contraction musculaire*, in *Editions Ar-sica*. 1956: Brussels, Belgium p. 315. 144
19. Hill, A.V., The effect of load on the heat of shortening. *Proc. Royal Soc. London. Ser. B. Biol. Sci.*, 1964. 159: 297–318. 144
20. Lymn, R.W. and E.W. Taylor, Mechanism of adenosine triphosphate hydrolysis by actomyosin. *Biochemistry*, 1971. 10: 4617–4624. 145, 151
21. Eisenberg, E. and L.E. Greene, The relation of muscle biochemistry to muscle physiology. *Annu Rev Physiol*, 1980. 42: 293–309. 145, 146
22. Pate, E. and R. Cooke, A model of crossbridge action: the effects of ATP, ADP and Pi. *J Muscle Res Cell Motil*, 1989. 10: 181–196. 145
23. Huxley, A.F., A note suggesting that the cross-bridge attachment during muscle contraction may take place in two stages. *Proc R Soc Lond B Biol Sci*, 1973. 183: 83–86. 145
24. Hill, T.L., Theoretical formalism for the sliding filament model of contraction of striated muscle. Part I. *Prog Biophys Mol Biol*, 1974. 28: 267–340.
25. Hines, M. and J.J. Blum, Bend propagation in flagella. I. Derivation of equations of motion and their simulation. *Biophys J*, 1978. 23: 41–57. 146
26. Hines, M. and J.J. Blum, Bend propagation in flagella. II. Incorporation of dynein cross-bridge kinetics into the equations of motion. *Biophys J*, 1979. 25: 421–441. 146
27. Brokaw, C.J. and D. Rintala, Computer simulation of flagellar movement. V. oscillation of cross-bridge models with an ATP-concentration-dependent rate function. *J Mechanochem Cell Motil*, 1977. 4: 205–232. 147
28. Brokaw, C.J., Models for oscillation and bend propagation by flagella. *Symp Soc Exp Biol*, 1982. 35: 313–338. 147
29. Sheetz, M.P. and J.A. Spudich, Movement of myosin-coated fluorescent beads on actin cables in vitro. *Nature*, 1983. 303: 31–35. 148
30. Spudich, J.A., S.J. Kron, and M.P. Sheetz, Movement of myosin-coated beads on oriented filaments reconstituted from purified actin. *Nature*, 1985. 315: 584–586. 148
31. Howard, J., A.J. Hudspeth, and R.D. Vale, Movement of microtubules by single kinesin molecules. *Nature*, 1989. 342: 154–158. 148
32. Uyeda, T.Q., S.J. Kron, and J.A. Spudich, Myosin step size. Estimation from slow sliding movement of actin over low densities of heavy meromyosin. *J Mol Biol*, 1990. 214: 699–710. 148, 149
33. Cox, R.G., The motion of long slender bodies in a viscous fluid. Part 1. General theory. *J. Fluid. Mech.*, 1970. 44: 791–810. 148
34. Pate, E. and R. Cooke, Simulation of stochastic processes in motile crossbridge systems. *J Muscle Res Cell Motil*, 1991. 12: 376–393. 151